J Therm Anal Calorim (2017) 129:1291–1299
DOI 10.1007/s10973-017-6296-2

Effects of some nucleating agents on the supercooling of erythritol to be applied as phase change material

Ju-Lan Zeng[1] · Lei Zhou[1] · Yue-Fei Zhang[1] · Sai-Ling Sun[1] · Yu-Hang Chen[1] · Li Shu[1] · Lin-Ping Yu[1] · Ling Zhu[1] · Liu-Bin Song[1] · Zhong Cao[1]

Received: 9 January 2017 / Accepted: 9 March 2017 / Published online: 20 March 2017

Abstract Nine nucleating agents, calcium pimelate (CaPi), bicyclic [1, 2, 2]heptane di-carboxylate (HPN-68), a commercially obtained aryl amide nucleating agent (TMB-5), calcium salt of hexahydrophthalic acid (HPN-20E), 1,3:2,4-di-p-methylbenzylidene sorbitol (MDBS) and sodium, potassium, magnesium and calcium salt of benzene-1, 3, 5-tricarboxylic acid (Na_3BTC, K_3BTC, Mg_3BTC_2 and Ca_3BTC_2, respectively), were applied to reduce the supercooling of erythritol, and their effects were investigated by cyclic differential scanning calorimetry (DSC). The results revealed that Na_3BTC and K_3BTC could not induce erythritol to crystallize under the experiment condition. MDBS could only make erythritol to crystallize at a temperature slightly higher than that of pure erythritol, and the effect was unstable. Mg_3BTC_2, Ca_3BTC_2 and HPN-68 could induce erythritol to crystallize at relatively high temperature, but the peak temperature of crystallizing ($T_{p,\ cr}$) and the phase change enthalpy of crystallizing ($\Delta_{cr}H$) decreased greatly as the melting–crystallizing cycles increased. HPN-20E-doped erythritol crystallized at a high temperature with the $T_{p,\ cr}$ of 69.3 °C at the first cycle, but the $T_{p,\ cr}$ and $\Delta_{cr}H$ varied greatly during the melting–crystallizing cycles. CaPi and TMB-5 could induce erythritol to crystallize at a stable temperature with the $T_{p,\ cr}$ of about 69 °C and 64 °C, respectively, and with a stable $\Delta_{cr}H$ of about 204 and 185 J g^{-1}, respectively, in all melting–crystallizing cycles. Hence, CaPi- and TMB-5-doped erythritol could be used as PCMs and applied in thermal energy storage in which the energy was absorbed at a high temperature and released at a lower but stable temperature.

Keywords Phase change material · Erythritol · Supercooling · Nucleating agents · Thermal energy storage

Introduction

Solar energy is one of the most well-known renewable energy due to its cleanness and inexhaustibility [1, 2]. However, solar irradiation is largely dependent on climate and would further fluctuate daily and seasonally; hence, results in energy storage units are indispensible in solar energy application system. Thermal energy storage has drawn more and more attention for decades due to the fact that it can solve the mismatch between the intermittent supplying and the continuous demanding for energy [3–5]. As a result, it plays an important role in renewable energy development, improving energy efficiency, and hence in favorable to solve the environment crisis caused by excessive utilization of fossil fuel. Phase change materials (PCMs) might be one of the best working medium in the thermal energy storage unit because they can absorb or release large amounts of thermal energy in a small temperature range just by changing their phases. Furthermore, solid–liquid PCMs should be one of the best choice as far as the thermal energy storage capacity, the volume changing, as well as the phase change dynamics are concerned [3]. A lot of solid–liquid PCMs could store thermal energy that comes from solar irradiation have been reported [6–12].

✉ Ju-Lan Zeng
julan_zeng@163.com

[1] Collaborative Innovation Center of Micro/Nano Bio-sensing and Food Safety Inspection, Hunan Provincial Key Laboratory of Materials Protection for Electric Power and Transportation, School of Chemistry and Biological Engineering, Changsha University of Science and Technology, Changsha 410114, People's Republic of China

Erythritol, a polyalcohol artificial sweeter, has been investigated as PCM in solar hot water supplying and solar absorption chilling system due to its relative high melting point (~118 °C) and very large melting latent heat (~350 J g^{-1}). Besides, it is environmental friendly, non-flammable, non-corrosive and low toxicity [13] and can be mass-produced with relative low degradation when used repeatedly [14]. However, it could undergo severe supercooling more than 100 °C [15]. Up till now, supercooling as a thermodynamic phenomenon is still not clearly understood [16]. Supercooling could vary greatly due to a lot of factors such as mass and volume size of the sample, impurities, agitations during cooling, containers and cooling conditions [17, 18], or even no factor at all [16]. As a result, the absorbed thermal energy in the molten PCMs might be released at an unacceptably large working temperature range rather than at a desired or constant temperature. Thus, it is important to relax the supercooling and make the molten PCMs crystallize at a temperature as close as possible to their melt point or at a constant temperature. Some methods such as ultrasound [15, 17] and addition of different polyalcohol [13] have been applied to relax the supercooling of erythritol. It was also reported that the supercooling of erythritol could be suppressed by graphitic structures with ultrahigh specific surface area [19].

On the other hand, adding nucleating agents is one of the most widespread and leading technique that researchers adopted to suppress the supercooling of PCMs [20–23]. Nucleating agents are solid particles or crystals added to PCMs and can induce the PCMs to crystallize but do not dissolve at the operational temperature. Application of nucleating agents to reduce the supercooling of PCMs was systematically summarized by Safari et al. [22]. However, to the best of our knowledge, no nucleating agent has been applied to relax the supercooling of sugar alcohol.

In the present work, nine kinds of substances, namely calcium pimelate (CaPi) [24], bicyclic [1, 2, 2] heptane dicarboxylate (commercially named as HPN-68) [25], a commercially obtained aryl amide nucleating agent (commercially named as TMB-5) [26], calcium salt of hexahydrophthalic acid (commercially named as HPN-20E) [27], 1,3:2,4-di-p-methylbenzylidene sorbitol (MDBS) [28] and sodium, potassium, magnesium and calcium salt of benzene-1, 3, 5-tricarboxylic acid (Na_3BTC, K_3BTC, Mg_3BTC_2 and Ca_3BTC_2, respectively) [29], were applied as nucleating agents. Their effects on the supercooling of erythritol were investigated by cyclic DSC, and the results are reported here. These substances were selected due to that they exhibited good results in nucleating of some polymers [24–29], and erythritol showed polymer-like chain structure through intermolecular hydrogen bonds [30].

Experimental

Materials

HPN-68 (Milliken Chemical Co., USA), TMB-5 (Fine Chemicals Department of Shanxi Provincial Institute of Chemical, China), HPN-20E (Milliken Chemical Co., USA) and MDBS (Hubei Huabang Chemical Co., China) were obtained commercially. Other nucleating agents were prepared as follows: CaPi was prepared according to Ref. [24], while Na_3BTC and K_3BTC were synthesized by reacting benzene-1,3,5-tricarboxylic acid with NaOH or KOH in ethanol at 50 °C for 2 h, respectively [29]. Mg_3BTC_2 and Ca_3BTC_2 were synthesized by reacting sodium benzene-1,3,5-tricarboxylic acid with calcium chloride or magnesium chloride in ethanol at 70 °C for 2 h, respectively [29]. All reagents except the commercially obtained nucleating agents were of analytical grade, obtained commercially and used as received without any further purification.

Preparation of the nucleating agents doped erythritol

Nucleating agents, erythritol and certain amount of methanol which was about five times of erythritol (volume in mL to mass in g) were mixed in a mortar. The mixture was grounded until the methanol was almost evaporated. The procedure was repeated for two times. Afterward, the mixture was dried in oven at 60 °C for 4 h to obtain the nucleating agents doped erythritol. The ratio of nucleating agent to erythritol was fixed as 1 mass %.

Characterization

The supercooling and the thermal energy storage properties of the samples were characterized using differential scanning calorimetry (DSC, TA Instruments Q2000) by heating the samples to 140 °C and then cooling to 0 °C with the heating or cooling rate of 10 °C min^{-1} in nitrogen atmosphere, and this heating and cooling processes were repeated for ten cycles. Prior to use, the calorimeter was calibrated using the extrapolated onset temperature (T_m) of the melting of indium (156.6 °C) and the heat of fusion of indium (28.45 J g^{-1}) at a heating rate of 10 °C min^{-1}.

Results and discussion

Supercooling of the nucleating agents doped erythritol

The DSC curves of the nucleating agents doped erythritol and pure erythritol during the first cycle are depicted in

Fig. 1. The heating scans of the first cycle were started at 80 °C due to that erythritol in its stable form would only start to melt at a temperature higher than 110 °C. Upon heating, pure erythritol melted with the T_m and peak temperature ($T_{p,\ m}$) of 118.7 and 119.8 °C, respectively. The figure also showed that HPN-68-, HPN-20E-, CaPi-, TMB-5- and MDBS-doped erythritol exhibited similar melting phenomena with the T_m and $T_{p,\ m}$ of 116–122 and 118–124 °C, respectively. However, the DSC curves of K_3BTC-, Na_3BTC-, Mg_3BTC_2- and Ca_3BTC_2-doped erythritol exhibited multi-peaks. The peak exhibited at $T_{p,\ m}$ of 114–119 °C was originated from the melting of erythritol, while the other peaks exhibited at lower temperature might be caused by that the nucleating agents were not pure enough and the un-reacted BTC would form eutectic mixture with erythritol. On the other hand, the cooling curves varied greatly. Erythritol showed a weak exothermic peak with the extrapolated onset temperatures (T_{cr}) of 19.8 °C and the peak temperature ($T_{p,\ cr}$) of 16.3 °C on its cooling curve, indicating that it exhibited great supercooling and could not be fully crystallized under the experimental condition. The Na_3BTC- and K_3BTC-doped erythritol did not show any exothermic peak on their cooling curves, indicating that both Na_3BTC and K_3BTC could not relax the supercooling of erythritol. The MDBS-doped erythritol showed a weak exothermic peak with the $T_{p,\ cr}$ of 23.4 °C, indicating that MDBS could only slightly relax the supercooling of erythritol. All other nucleating agents doped erythritol showed a exothermic peak, which was corresponding to the crystallizing of liquid erythritol, on their cooling DSC curves at a temperature obviously higher than that of pure erythritol, indicating that they all could suppress the supercooling of erythritol to some extent.

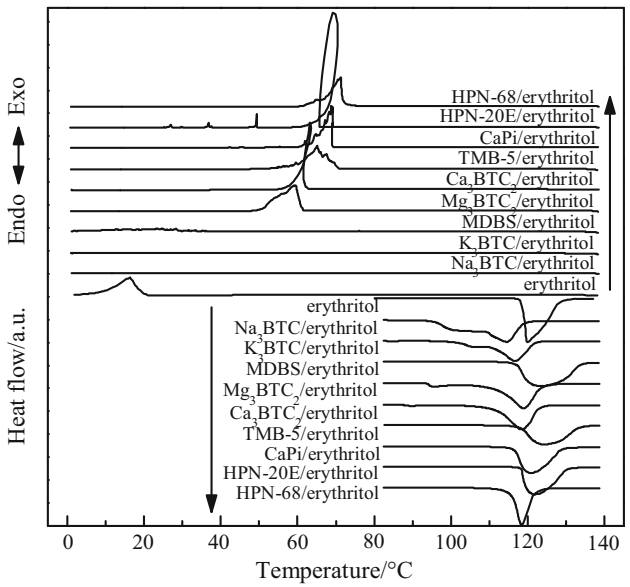

Fig. 1 Heating and cooling DSC curves of pure and nucleating agents doped erythritol at the first DSC cycle

It could be seen from Fig. 1 that a loop was exhibited in some cooling DSC curves. The DSC instrument used here is a heat flux-type DSC which measures the temperature of the sample and the reference and then obtains the heat flux based on the temperature difference between the sample and the reference. If a sample exhibits supercooling and is cooled from liquid, the temperature of the sample would drop to a temperature lower than its melting point without crystallizing. When the crystallization starts, great amounts of heat would be released and resulted in a temperature rising of the sample. Hence, a loop would be exhibited. The T_{cr} of these samples was obtained as follows: The DSC curves were drawn using time as x-axis (the x-axis of the DSC curves that shown in this paper was set as temperature in order to compare the supercooling) and the extrapolated onset time could be obtained, and then, the T_{cr} was obtained according to the extrapolated onset time and the temperature of the sample. The melting and the solidifying of erythritol are overlap of various components [31], and for such kind of materials, it is believed that $T_{p,cr}$ and $T_{p,m}$ are more accurate and more easily to be determined [31]. Hence, the extent of supercooling, ΔT, was defined as the difference between the $T_{p,\ m}$ and $T_{p,\ cr}$. The T_m, T_{cr}, $T_{p,\ m}$, $T_{p,\ cr}$ and ΔT of pure erythritol and the nucleating agents doped erythritol during ten DSC cycles are listed in Table 1. It could be seen from the data of the first cycle that erythritol exhibited the largest ΔT of 103.5 °C, while the ΔT of the nucleating agents, except Na_3BTC- and K_3BTC-doped erythritol, was in the range of 47–100 °C, of which HPN-68, HPN-20E, CaPi and TMB-5 showed the best results on suppressing the supercooling of erythritol. The ΔT of the HPN-68-, HPN-20E-, CaPi- and TMB-5-doped erythritol was 47.1, 52.3, 52.1 and 59.3 °C, respectively. It could also be seen from the data that, in all ten DSC cycles, both Na_3BTC and K_3BTC did not show any effect on relaxing the supercooling of erythritol, and the MDBS-doped erythritol also did not exhibit significant decrease in supercooling. As a result, these composites would be excluded from further evaluation.

Supercooling relaxation stability of the nucleating agents doped erythritol

Upon cooling from liquid state, erythritol could form unstable solid phase which would melt at about 104 °C [31]. Hence, both $T_{p,\ cr}$ and ΔT should be considered and $T_{p,\ cr}$ should be the more important parameter when the relaxation of supercooling of erythritol was discussed. The $T_{p,\ cr}$ of every cycle of pure erythritol and the nucleating agents doped erythritol are depicted in Fig. 2. It could be found that the $T_{p,\ cr}$ of erythritol varied in the range of

Table 1 T_m, T_{cr}, $T_{p,\ m}$, $T_{p,\ cr}$ and ΔT of pure and nucleating agents doped erythritol obtained by DSC measurement

Erythritol with nucleating agent/°C	Cycles									
	1	2	3	4	5	6	7	8	9	10
Erythritol										
T_m	118.67	118.37	118.62	118.72	118.71	118.59	118.69	118.59	118.71	118.5
T_{cr}	19.21	15.99	11.72	12.38	18.58	14.46	17.55	15.92	16.13	15.67
$T_{p,\ m}$	119.82	121.8	122.08	122.11	122.14	122.47	122.49	122.5	122.52	122.25
$T_{p,\ cr}$	16.32	10.02	7.37	7.07	13.63	10.55	12.99	12.02	15.15	10.92
ΔT	103.5	111.78	114.71	115.04	108.51	111.92	109.5	110.48	107.37	111.33
HPN-68/erythritol										
T_m	115.88	102.32	101.7	114.4	101.01	100.68	100.32	100.01	99.66	98.83
T_{cr}	71.65	66.07	73.96	68.56	65.46	68.46	67.21	65.36	68.02	60.96
$T_{p,\ m}$	118.31	104.86	104.62	116.84	104.3	104.14	104.03	103.92	103.87	103.58
$T_{p,\ cr}$	71.25	65.18	66.93	63.03	61.88	56.29	60.02	56.25	57.4	54.49
ΔT	47.06	39.68	37.69	53.81	43.42	47.85	44.01	47.67	46.47	49.09
HPN-20E/erythritol										
T_m	118.32	118.29	118.26	118.32	118.35	118.41	118.55	118.64	118.64	118.66
T_{cr}	65.79	49.69	55.09	57.52	54.15	54.98	55.51	51.26	53.77	57.38
$T_{p,\ m}$	121.63	121.03	121.11	121.2	121.29	121.4	121.52	121.51	121.54	121.54
$T_{p,\ cr}$	69.33	52.83	58.55	60.49	56.71	57.51	58.61	53.04	56.31	60.05
ΔT	52.3	68.2	62.56	60.71	64.58	63.89	62.91	68.47	65.23	61.49
CaPi/erythritol										
T_m	116.51	100.49	101.61	102.37	102.9	103.32	103.65	103.97	104.25	104.49
T_{cr}	68.96	68.82	68.46	66.62	68.78	66.99	67.95	68.35	66.34	64.41
$T_{p,\ m}$	120.97	106.05	105.93	106.12	106.29	106.5	106.67	106.87	106.94	107.02
$T_{p,\ cr}$	68.89	68.93	69.69	69.78	70.32	69.91	70.25	69.85	69.12	65.96
ΔT	52.08	37.12	36.24	36.34	35.97	36.59	36.42	37.02	37.82	41.06
TMB-5/erythritol										
T_m	118.19	118.18	118.16	118.16	118.18	118.2	118.16	118.24	118.21	118.24
T_{cr}	67.33	69.53	63.91	63.61	62.73	63.9	63.01	63.7	63.03	62.79
$T_{p,\ m}$	124.38	124.38	124.35	124.41	124.43	124.44	124.43	124.43	124.46	124.39
$T_{p,\ cr}$	65.13	66.98	63.64	63.02	62.91	63.82	62.8	63.4	62.88	63.52
ΔT	59.25	57.4	60.71	61.39	61.52	60.62	61.63	61.03	61.58	60.87
Ca_3BTC_2/erythritol										
T_m	111.49	100.82	101.2	101.58	101.84	102.06	102.38	102.58	102.3	102.96
T_{cr}	61.64	58.29	57.15	58.42	56.14	57.70	56.87	49.86	49.76	47.27
$T_{p,\ m}$	118.33	105.8	105.88	105.93	106.14	106.23	106.33	106.36	106.19	106.5
$T_{p,\ cr}$	63.34	57.75	56.95	57.85	56.57	57.71	55.92	49.9	49.65	47.84
ΔT	54.99	48.05	48.93	48.08	49.57	48.52	50.41	56.46	56.54	58.66
Mg_3BTC_2/erythritol										
T_m	111.87	100.71	101.28	101.71	102.13	102.52	102.76	103.03	116.16	116.13
T_{cr}	60.64	57.96	54.41	58.48	56.47	54.1	47.05	48.28	44.41	46.42
$T_{p,\ m}$	118.82	106.82	107.05	107.25	107.5	107.62	107.8	107.88	120.51	120.48
$T_{p,\ cr}$	59.6	54.33	51.68	53.47	50.42	47.4	46.31	45.59	43.71	45.79
ΔT	59.22	52.49	53.37	53.78	57.08	60.22	61.49	62.29	76.8	74.69
MDBS/erythritol										
T_m	117.37	117.97	117.69	117.61	117.52	117.56	117.61	117.63	117.73	117.8
T_{cr}	29.14	23.91	28.36	30.92	24.89	25.2	25.35	23.6	17.56	21.96
$T_{p,\ m}$	123.45	123.34	123.66	123.72	123.87	123.92	123.85	123.84	123.9	123.9
$T_{p,\ cr}$	23.39	23.28	27.73	18.12	22.29	16.98	25.06	14.63	16.63	18.63

Table 1 continued

Erythritol with nucleating agent/°C	Cycles									
	1	2	3	4	5	6	7	8	9	10
ΔT	100.06	100.06	95.93	105.6	101.58	106.94	98.79	109.21	107.27	105.27
K_3BTC/erythritol										
T_m	110.28	110.39	111.06	111.74	112.1	112.33	112.44	112.64	112.69	112.8
T_{cr}	NA	NA	NA	NA	NA	NA	NA	NA	NA	NA
$T_{p,\ m}$	116.63	116.84	117.31	117.5	117.68	117.77	117.9	117.99	118.04	118.11
$T_{p,\ cr}$	NA	NA	NA	NA	NA	NA	NA	NA	NA	NA
ΔT	NA	NA	NA	NA	NA	NA	NA	NA	NA	NA
Na_3BTC/erythritol										
T_m	106.11	104.62	104.78	105.04	105.48	105.63	105.91	106.03	106.23	106.49
T_{cr}	NA	NA	NA	NA	NA	NA	NA	NA	NA	NA
$T_{p,\ m}$	114.49	114.32	114.34	114.42	114.46	114.55	114.53	114.68	114.72	114.75
$T_{p,\ cr}$	NA	NA	NA	NA	NA	NA	NA	NA	NA	NA
ΔT	NA	NA	NA	NA	NA	NA	NA	NA	NA	NA

$\Delta T = T_{p,\ m} - T_{p,\ cr}$, *NA* not available

16.3–7.1 °C, which is common for supercooling phenomena. The $T_{p,\ cr}$ of HPN-20E-doped erythritol was greatly and also randomly varied, indicating that it might not be a suitable candidate nucleating agent for erythritol. On the other hand, the $T_{p,\ cr}$ of HPN-68-, Ca_3BTC_2- and Mg_3BTC_2-doped erythritol exhibited a severe tendency of decreasing as the melting–crystallizing cycles increased, indicating that the effect of the relaxation of supercooling was decreased, which might be the result of the precipitation of the nucleating agent. However, the $T_{p,\ cr}$ of CaPi- and TMB-5-doped erythritol was stable in all ten melting–crystallizing cycles, indicating that they could induce erythritol to stably crystallize at the corresponding temperature.

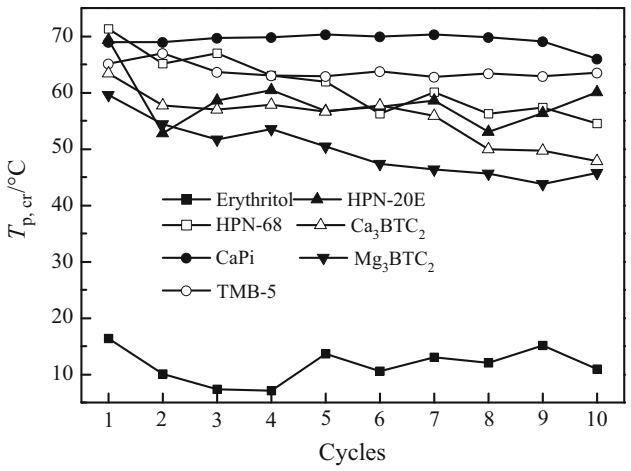

Fig. 2 $T_{p,cr}$ of pure and nucleating agents doped erythritol at each melting–crystallizing cycles. The legends in the figure, except erythritol, represent the corresponding nucleating agents doped erythritol

Then, we checked the cyclic DSC curves of erythritol and CaPi-, HPN-68-, HPN-20E- and TMB-5-doped erythritol. The cyclic DSC curves of erythritol are drawn in Fig. 3. The figure, along with the data listed in Table 1, revealed that erythritol always melted at about 118 °C. However, the cooling curves revealed that its crystallizing behavior varied greatly from cycle to cycle. Besides, the end of most cooling curves did not go back to the base line, and there were some exothermic peaks, which was caused by cold crystallization, exhibited on all the heating curves except the first heating curve, indicating that erythritol could not finish its crystallization under the experiment condition.

On the other hand, the cyclic DSC curves of the CaPi-doped erythritol (Fig. 4) and the corresponding data in Table 1 showed that it always melted at about 104 °C in all heating runs after the first cycle, indicating that CaPi could induce erythritol to form unstable crystals under the experiment condition. The cooling DSC curves were very similar and an exothermic peak with the $T_{p,cr}$ of about 69 °C was exhibited on all curves. No exothermic peak could be found on the heating DSC curves of the CaPi-doped PCMs. It further approved that CaPi possessed stable effect on suppressing the supercooling of erythritol.

As for the TMB-5-doped erythritol, the cyclic DSC curves (Fig. 5) and the data in Table 1 revealed that it always melted at about 120 °C. However, there were a small exothermic peak, corresponding to the cold crystallization of erythritol, and a small endothermic peak, corresponding to the melting of unstable solid phase [31],

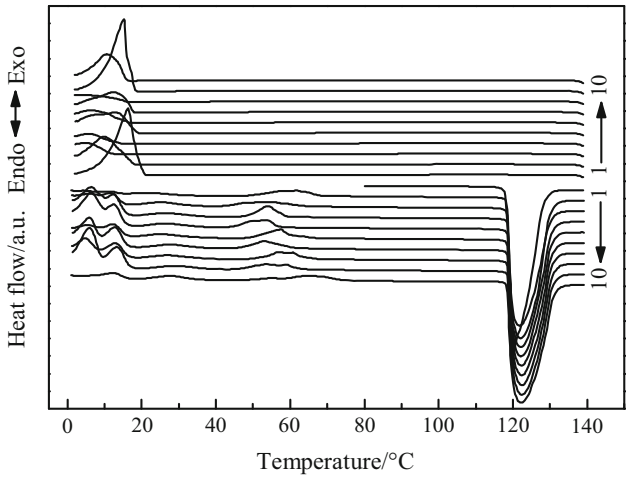

Fig. 3 Cyclic DSC curves of erythritol

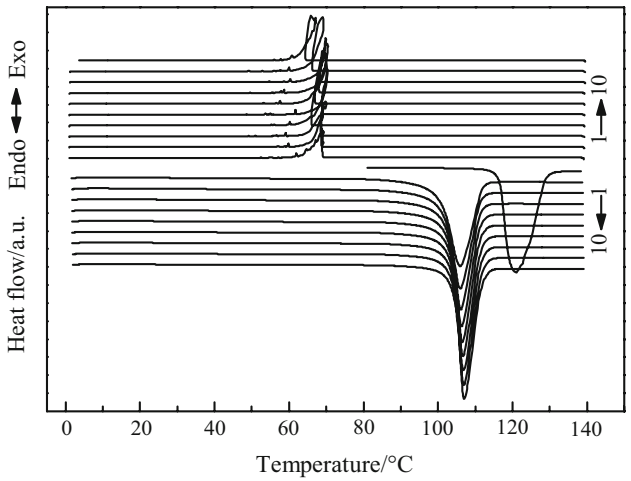

Fig. 4 Cyclic DSC curves of CaPi-doped erythritol

exhibited on all heating DSC curves at a nearly constant temperature except the first cycle. These phenomena suggested that, up on cooling, TMB-5 could induce erythritol to form both stable and unstable solid phases and the stable phase is the majority. On the other hand, the cooling curves of TMB-5-doped erythritol were very similar after the second cycle, and the exothermic peaks were located at about 60 °C, indicating that TMB-5 also possessed stable effect on relaxing the supercooling of erythritol, although its $T_{p,cr}$ was a little bit lower than that of CaPi-doped erythritol.

The cyclic DSC curves of the HPN-68-doped erythritol (Fig. 6) and the data in Table 1 showed that it would melt at 104 or 118 °C, indicating that the composite could form stable or unstable phase upon crystallizing. Besides, no exothermic peak could be found on the heating DSC curves, which means that the crystallized product was stable under the experimental condition. However, the

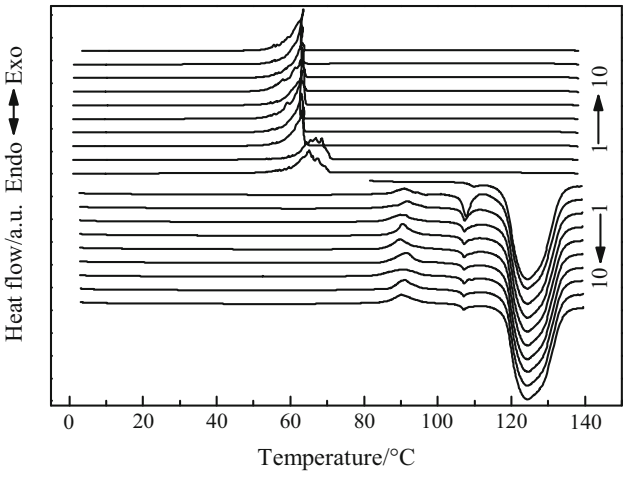

Fig. 5 cyclic DSC curves of TMB-5-doped erythritol

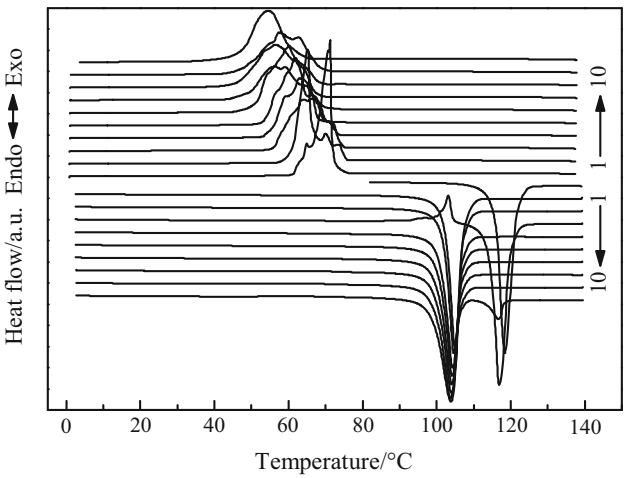

Fig. 6 Cyclic DSC curves of HPN-68-doped erythritol

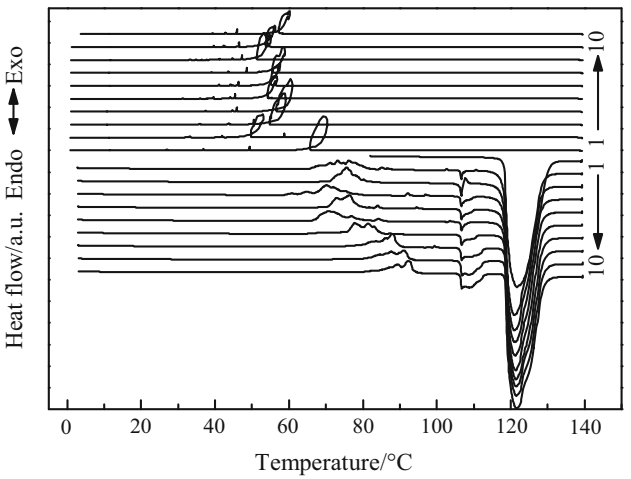

Fig. 7 Cyclic DSC curves of HPN-20E-doped erythritol

exothermic peaks of the cooling DSC curves were continually moved to lower temperature as the melting–crystallizing cycles increased. It further suggested that the supercooling relaxation of HPN-68 on erythritol would decrease as the melting–crystallizing cycles increased.

On the other hand, the cyclic DSC curves of the HPN-20E-doped erythritol (Fig. 7) revealed that it would mainly melted at about 118 °C. However, there were some relatively large exothermic peaks randomly exhibited on all heating DSC curves after the first melting–crystallizing cycle, indicating that it would randomly cold crystallize at different temperature. Besides, endothermic peaks corresponding to the melting of unstable solid phase were also shown on all heating DSC curves after the first melting–crystallizing cycle and the area of the peak also varied randomly. These phenomena further confirmed that HPN-20E might not be a suitable candidate nucleating agent for the supercooling relaxation of erythritol.

Thermal energy storage properties of the nucleating agents doped erythritol

The phase change enthalpy of melting ($\Delta_m H$) and crystallizing ($\Delta_{cr} H$) of erythritol and the nucleating agents doped erythritol obtained by ten cyclic DSC are listed in Table 2, and the $\Delta_{cr} H$ of erythritol and the nucleating agents doped erythritol at each cycle are depicted in Fig. 8. It could be seen that the $\Delta_m H$ of erythritol was stabilized at about 350 J g^{-1}, which is agreed well with Ref. [32]. However, because of its serious supercooling, its $\Delta_{cr} H$ drastically

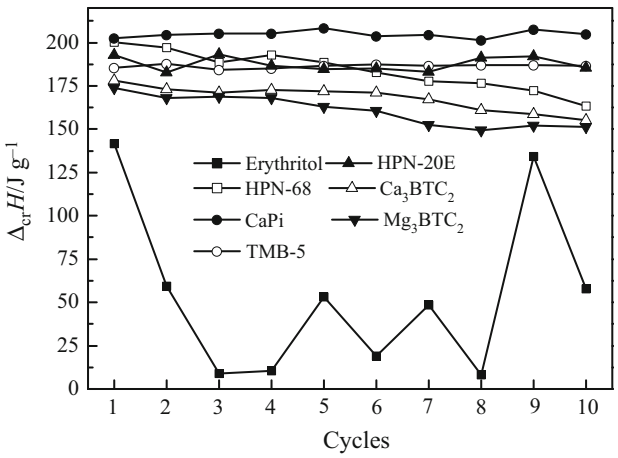

Fig. 8 $\Delta_{cr} H$ of pure and nucleating agents doped erythritol at each melting–crystallizing cycles. The legends in the figure, except erythritol, represent the corresponding nucleating agents doped erythritol

Table 2 $\Delta_m H$ and $\Delta_{cr} H$ of pure and nucleating agents doped erythritol obtained by DSC measurement

Erythritol with nucleating agent/J g^{-1}	Cycles									
	1	2	3	4	5	6	7	8	9	10
Erythritol										
$\Delta_m H$	357.3	357.2	357.1	354.7	353.0	353.5	353.3	353.8	353.7	354.3
$\Delta_{cr} H$	141.8	59.48	9.01	10.48	53.29	18.92	48.51	8.011	134.4	57.65
HPN-68/erythritol										
$\Delta_m H$	270.3	232.0	221.4	264.3	217.4	220.7	220.0	217.1	211.3	211.9
$\Delta_{cr} H$	200.3	197.1	188.6	192.8	188.4	182.7	177.7	176.7	172.4	163.3
HPN-20E/erythritol										
$\Delta_m H$	288.3	280.5	277.7	279.8	278.6	276.6	279.7	280.3	278.5	277.0
$\Delta_{cr} H$	192.8	182.6	193.3	186.5	184.5	185.2	183.3	191.2	191.9	185.6
CaPi/erythritol										
$\Delta_m H$	288.7	237.8	225.8	232.2	237.7	239.9	242.9	237.7	242.4	248.9
$\Delta_{cr} H$	202.7	204.3	205.4	205.1	208.2	203.6	204.4	201.2	207.6	204.7
TMB-5/erythritol										
$\Delta_m H$	254.7	236.1	232.1	232.4	225.6	231.5	241.2	227.7	234.8	229.8
$\Delta_{cr} H$	185.3	187.9	184.4	184.9	186.8	187.3	186.6	187.2	187.1	186.8
Ca_3BTC_2/erythritol										
$\Delta_m H$	218.5	210.2	213.1	215.3	210.4	215.1	212.1	218.1	225.2	218.7
$\Delta_{cr} H$	178.2	173.2	171.0	172.6	171.8	171.1	167.4	161.2	158.8	155.2
Mg_3BTC_2/erythritol										
$\Delta_m H$	256.7	209.7	213.2	215.6	220.0	220.6	222.4	219.1	245.7	246.2
$\Delta_{cr} H$	174.0	168.1	168.6	168.0	163.1	160.6	152.6	149.3	152.0	151.2

varied from cycle to cycle, and sometimes, it was unacceptably low. For example, the $\Delta_{cr}H$ of cycle 8 was only 8.01 J g^{-1}. It further confirmed that erythitol might cannot finish its crystallization under the experiment condition.

When HPN-68 was applied as nucleating agent, its Δ_mH of the first heating run was also the largest. But the Δ_mH of the fourth heating run was very close to the first one. It could be ascribed to that, during the fourth heating run, it was the stable solid phase to melt, which could be approved by the T_m. The Δ_mH of those heating runs in which it was the unstable solid phase to melt was obviously lower than that of the first and the fourth heating runs. Besides, the data in Table 2 and Fig. 8 showed that the $\Delta_{cr}H$ of the HPN-68 doped erythritol decreased obviously as the melting–crystallizing cycles increased, from 200.3 to 163.3 J g^{-1}, suggesting that it could not be applied as good PCM. The figure also showed that the $\Delta_{cr}H$ of Ca_3BTC_2- and Mg_3BTC_2-doped erythritol also decreased obviously from about 175 to about 150 J g^{-1} during the ten melting–crystallizing cycles. Since their $T_{p,\ cr}$ was also greatly decreased during the ten cycles, it seems that, although their Δ_mH was relatively high, Ca_3BTC_2 and Mg_3BTC_2 were not good nucleating agents for erythritol. The Δ_mH of HPN-20E-doped erythritol was relatively high and stabilized at about 280 J g^{-1}. However, its $\Delta_{cr}H$ was varied a lot during the ten melting–crystallizing cycles, plus its greatly varied $T_{p,\ cr}$, it could not to be viewed as a suitable PCM.

When CaPi was applied as nucleating agent, the Δ_mH of the first heating was 288.7 J g^{-1} with the T_m of 116.5 °C. The Δ_mH was lower than the value calculated from the loading of erythritol in the doped PCM, suggesting that some erythritol lost its phase change ability due to the doping of CaPi. The Δ_mH of the CaPi-doped erythritol after the first cycle was varied from 226 to 249 J g^{-1} with the T_m varied between 101 and 104 °C. The Δ_mH was lower than that of the first heating because it was the unstable solid phase to melting and absorbs energy after the first cycle. On the other hand, it could be seen from Fig. 8 that the $\Delta_{cr}H$ of the CaPi-doped erythritol was highly stabilized in the range of 201–208 J g^{-1} in all cooling runs. The T_m of the TMB-5-doped PCM was stabilized at ~118 °C, and it also showed a larger Δ_mH of 254.7 J g^{-1} at the first heating run and then followed by relatively stable Δ_mH in the range of 227–241 J g^{-1} at all the following heating runs. The difference of Δ_mH between the first and the afterward heating runs could be ascribed to the small endothermic peaks exhibited at about 104 °C, which was resulted from the melting of the unstable solid phase. Furthermore, it could be found from Fig. 8 and Table 2 that the $\Delta_{cr}H$ of the TMB-5-doped erythritol, which was in the range of 185–188 J g^{-1}, was very stable in all ten melting–crystallizing cycles.

In general, both the Δ_mH and $\Delta_{cr}H$ of the CaPi- and TMB-5-doped erythritol were very high comparing to most organic PCMs such as fatty acids, wax and polyethylene glycol [33]. Since the CaPi- and TMB-5-doped erythritol could melt and crystallize at nearly constant temperature and possess stable and high phase change enthalpy, they could be viewed as good PCMs and applied in thermal energy storage in which the energy was absorbed at a temperature higher than 120 °C and then released at a lower but stable temperature.

Conclusions

The relaxation of nine nucleating agents on the supercooling of erythritol was investigated by cyclic DSC experiment. The supercooling of pure erythritol was higher than 100 °C in all melting–crystallizing cycles and varied greatly from cycle to cycle. K_3BTC and Na_3BTC could not induce erythritol to crystallize in the experiment condition. MDBS could only make erythritol to crystallize at a temperature slightly higher than that of pure erythritol with a very small $\Delta_{cr}H$, and the $T_{p,\ cr}$ also varied greatly. Both the Mg_3BTC_2- and Ca_3BTC_2-doped erythritol could crystallized at a relatively high temperature with the $T_{p,\ cr}$ of 60 and 63 °C, respectively, but their $T_{p,\ cr}$ and $\Delta_{cr}H$ decreased greatly as the melting–crystallizing cycles increased. HPN-68-doped erythritol exhibited the best result on suppressing the supercooling at the first melting–crystallizing cycle, but both of its $T_{p,\ cr}$ and $\Delta_{cr}H$ drastically decreased as the melting–crystallizing cycles increased. HPN-20E-doped erythritol could crystallized at a high temperature with the $T_{p,\ cr}$ of 69.3 °C, but its $T_{p,\ cr}$ and $\Delta_{cr}H$ varied a lot during the afterward melting–crystallizing cycles, made it unsuitable for real application. CaPi- and TMB-5-doped erythritol could crystallize at higher temperature with the $T_{p,\ cr}$ stabilized at about 69 and 64 °C, respectively, in all melting–crystallizing cycles. Furthermore, their $\Delta_{cr}H$ was also stabilized at about 204 and 185 J g^{-1}, respectively. Hence, CaPi- and TMB-5-doped erythritol could be used as PCMs and applied in thermal energy storage in which the energy was absorbed at a temperature higher than 120 °C and released at a lower but stable temperature. Further investigations of the mechanism of the supercooling suppression are under way.

Acknowledgements The authors gratefully acknowledge the financial support from the National Natural Science Foundation of China (21003014, 21376031, 21501015 and 21275022), the Natural Science Foundation of Hunan Province, China (2017JJ1026, 13JJ3068), Scientific Research Fund of Hunan Provincial Education Department (15B0002) and the Hunan Provincial Key Laboratory of Materials Protection for Electric Power and Transportation (Changsha University of Science and Technology) (2014CL05).

References

1. Barlev D, Vidu R, Stroeve P. Innovation in concentrated solar power. Sol Energy Mater Sol Cells. 2011;95(10):2703–25.
2. Aman MM, Solangi KH, Hossain MS, Badarudin A, Jasmon GB, Mokhlis H, et al. A review of safety, health and environmental (SHE) issues of solar energy system. Renew Sustain Energy Rev. 2015;41:1190–204. doi:10.1016/j.rser.2014.08.086.
3. Su W, Darkwa J, Kokogiannakis G. Review of solid–liquid phase change materials and their encapsulation technologies. Renew Sustain Energy Rev. 2015;48:373–91. doi:10.1016/j.rser.2015.04.044.
4. Pintaldi S, Perfumo C, Sethuvenkatraman S, White S, Rosengarten G. A review of thermal energy storage technologies and control approaches for solar cooling. Renew Sustain Energy Rev. 2015;41:975–95. doi:10.1016/j.rser.2014.08.062.
5. Khadiran T, Hussein MZ, Zainal Z, Rusli R. Encapsulation techniques for organic phase change materials as thermal energy storage medium: a review. Sol Energy Mater Sol Cells. 2015;143:78–98. doi:10.1016/j.solmat.2015.06.039.
6. Z-j Duan, H-z Zhang, L-x Sun, Cao Z, Xu F, Y-j Zou, et al. CaCl2·6H2O/expanded graphite composite as form-stable phase change materials for thermal energy storage. J Therm Anal Calorim. 2014;115(1):111–7. doi:10.1007/s10973-013-3311-0.
7. Zhang HZ, Xu QY, Zhao ZM, Zhang J, Sun YJ, Sun LX, et al. Preparation and thermal performance of gypsum boards incorporated with microencapsulated phase change materials for thermal regulation. Sol Energy Mater Sol Cells. 2012;102:93–102. doi:10.1016/j.solmat.2012.03.020.
8. Zeng JL, Zheng SH, Yu SB, Zhu FR, Gan J, Zhu L, et al. Preparation and thermal properties of palmitic acid/polyaniline/exfoliated graphite nanoplatelets form-stable phase change materials. Appl Energy. 2014;115:603–9. doi:10.1016/j.apenergy.2013.10.061.
9. Zeng JL, Gan J, Zhu FR, Yu SB, Xiao ZL, Yan WP, et al. Tetradecanol/expanded graphite composite form-stable phase change material for thermal energy storage. Sol Energy Mater Sol Cells. 2014;127:122–8. doi:10.1016/j.solmat.2014.04.015.
10. Fernández AG, Galleguillos H, Fuentealba E, Pérez FJ. Thermal characterization of HITEC molten salt for energy storage in solar linear concentrated technology. J Therm Anal Calorim. 2015;122(1):3–9. doi:10.1007/s10973-015-4715-9.
11. Genc ZK, Canbay CA, Acar SS, Sekerci M, Genc M. Preparation and thermal properties of heterogeneous composite phase change materials based on camphene–palmitic acid. J Therm Anal Calorim. 2015;120(3):1679–88. doi:10.1007/s10973-015-4478-3.
12. Sádovská G, Honcová P, Pilař R, Oravová L, Honc D. Calorimetric study of calcium nitrate tetrahydrate and magnesium nitrate hexahydrate. J Therm Anal Calorim. 2016;124(1):539–46. doi:10.1007/s10973-015-5159-y.
13. Hidaka H, Yamazaki M, Yabe M, Kakiuchi H, Ona EP, Kojima Y, et al. New PCMs prepared from erythritol–polyalcohols mixtures for latent heat storage between 80 and 100 °C. J Chem Eng Jpn. 2004;37(9):1155–62. doi:10.1252/jcej.37.1155.
14. Adachi T, Daudah D, Tanaka G. Effects of supercooling degree and specimen size on supercooling duration of erythritol. ISIJ Int. 2014;54(12):2790–5. doi:10.2355/isijinternational.54.2790.
15. Ona EP, Zhang X, Kyaw K, Watanabe F, Matsuda H, Kakiuchi H, et al. Relaxation of supercooling of erythritol for latent heat storage. J Chem Eng Jpn. 2001;34(3):376–82. doi:10.1252/jcej.34.376.
16. Okawa S, Saito A, Minami R. The solidification phenomenon of the supercooled water containing solid particles. Int J Refrig. 2001;24(1):108–17. doi:10.1016/S0140-7007(00)00060-8.
17. Ona EP, Zhang X, Ozawa S, Matsuda H, Kakiuchi H, Yabe M, et al. Influence of ultrasonic irradiation on the solidification behavior of erythritol as a PCM. J Chem Eng Jpn. 2002;35(3):290–8. doi:10.1252/jcej.35.290.
18. Wei L, Ohsasa K. Supercooling and solidification behavior of phase change material. ISIJ Int. 2010;50(9):1265–9. doi:10.2355/isijinternational.50.1265.
19. Kholmanov I, Kim J, Ou E, Ruoff RS, Shi L. Continuous carbon nanotube-ultrathin graphite hybrid foams for increased thermal conductivity and suppressed subcooling in composite phase change materials. ACS Nano. 2015;9(12):11699–707. doi:10.1021/acsnano.5b02917.
20. Ushak S, Gutierrez A, Barreneche C, Fernandez AI, Grágeda M, Cabeza LF. Reduction of the subcooling of bischofite with the use of nucleatings agents. Solar Energy Mater Sol Cells. 2016;157:1011–8. doi:10.1016/j.solmat.2016.08.015.
21. Cui W, Yuan Y, Sun L, Cao X, Yang X. Experimental studies on the supercooling and melting/freezing characteristics of nano-copper/sodium acetate trihydrate composite phase change materials. Renew Energy. 2016;99:1029–37. doi:10.1016/j.renene.2016.08.001.
22. Safari A, Saidur R, Sulaiman FA, Xu Y, Dong J. A review on supercooling of phase change materials in thermal energy storage systems. Renew Sustain Energy Rev. 2017;70:905–19. doi:10.1016/j.rser.2016.11.272.
23. Al-Shannaq R, Kurdi J, Al-Muhtaseb S, Dickinson M, Farid M. Supercooling elimination of phase change materials (PCMs) microcapsules. Energy. 2015;87:654–62. doi:10.1016/j.energy.2015.05.033.
24. Li JX, Cheung WL. Pimelic acid-based nucleating agents for hexagonal crystalline polypropylene. J Vinyl Addit Technol. 1997;3(2):151–6. doi:10.1002/vnl.10182.
25. Zhang YF, Chang Y, Li X, Xie D. Nucleation effects of a novel nucleating agent bicyclic [1, 2, 2] heptane di-carboxylate in isotactic polypropylene. J Macromol Sci B. 2010;50(2):266–74. doi:10.1080/00222341003648995.
26. Liu H, Huo H. Crystal phases, structure, and orientation in isotactic polypropylene after isothermal crystallization under oscillatory shear as a function of nucleation agent. Colloid Polym Sci. 2014;292(4):849–61. doi:10.1007/s00396-013-3133-4.
27. Zhang YF, Guo LH, Chen H, Liu BB, Gu YH. Properties and crystallization behaviors of isotactic polypropylene under action of an effective nucleating agent. J Macromol Sci B. 2015;54(9):1019–28. doi:10.1080/00222348.2015.1060404.
28. Zhang YF. Comparison of nucleation effects of organic phosphorous and sorbitol derivative nucleating agents in isotactic polypropylene. J Macromol Sci B. 2008;47(6):1188–96. doi:10.1080/00222340802403412.
29. Zhang YF, Luo XZ. Effects of benzene-1, 3, 5-tricarboxylate salts on crystallization and melting behaviors of isotactic polypropylene. In: Prushotaman E, editor. 2013 international conference on biological, medical and chemical engineering. Hong Kong; 2013.
30. Ceccarelli C, Jeffrey GA, McMullan RK. A neutron diffraction refinement of the crystal structure of erythritol at 22.6 K. Acta Crystallogr B. 1980;36(12):3079–307983. doi:10.1107/S0567740880010825.
31. Lopes Jesus AJ, Nunes SCC, Ramos Silva M, Matos Beja A, Redinha JS. Erythritol: crystal growth from the melt. Int J Pharm. 2010;388(1–2):129–35. doi:10.1016/j.ijpharm.2009.12.043.
32. Domalski ES, Hearing ED. Heat capacities and entropies of organic compounds in the condensed phase. Volume III. J Phys Chem Ref Data. 1996;25(1):1–525. doi:10.1063/1.555985.
33. Zalba B, Marin JM, Cabeza LF, Mehling H. Review on thermal energy storage with phase change: materials, heat transfer analysis and applications. Appl Therm Eng. 2003;23(3):251–83.